Arabidopsis Responds to *Alternaria alternata* Volatiles by Triggering Plastid Phosphoglucose Isomerase-Independent Mechanisms[1][OPEN]

Ángela María Sánchez-López[2], Abdellatif Bahaji[2], Nuria De Diego[2], Marouane Baslam, Jun Li, Francisco José Muñoz, Goizeder Almagro, Pablo García-Gómez, Kinia Ameztoy, Adriana Ricarte-Bermejo, Ondřej Novák, Jan F. Humplík, Lukáš Spíchal, Karel Doležal, Sergio Ciordia, María Carmen Mena, Rosana Navajas, Edurne Baroja-Fernández, and Javier Pozueta-Romero*

Instituto de Agrobiotecnología, Consejo Superior de Investigaciones Científicas/UPNA/Gobierno de Navarra, 31192 Mutiloabeti, Nafarroa, Spain (A.M.S.-L., A.B., M.B., J.L., F.J.M., G.A., P.G.-G., K.A., A.R.-B., E.B.-F., J.P.-R.); Department of Chemical Biology and Genetics, Centre of the Region Haná for Biotechnological and Agricultural Research, Faculty of Science, Palacký University, Olomouc CZ–78371, Czech Republic (N.D.D., J.F.H., L.S., K.D.); Laboratory of Growth Regulators, Centre of the Region Haná for Biotechnological and Agricultural Research, Faculty of Science, Palacký University, and Institute of Experimental Botany AS CR, Olomouc CZ–78371, Czech Republic (O.N., K.D.); and Unidad de Proteómica Centro Nacional de Biotecnología, Consejo Superior de Investigaciones Científicas, Campus de Cantoblanco, Madrid 28049, Spain (S.C., M.C.M., R.N.)

ORCID IDs: 0000-0002-0426-2118 (F.J.M.); 0000-0003-2369-3690 (K.A.); 0000-0002-8915-4369 (J.F.H.); 0000-0003-4938-0350 (K.D.); 0000-0002-4481-0553 (R.N.); 0000-0003-0049-6045 (E.B.-F.); 0000-0002-0335-9663 (J.P.-R.).

Volatile compounds (VCs) emitted by phylogenetically diverse microorganisms (including plant pathogens and microbes that do not normally interact mutualistically with plants) promote photosynthesis, growth, and the accumulation of high levels of starch in leaves through cytokinin (CK)-regulated processes. In Arabidopsis (*Arabidopsis thaliana*) plants not exposed to VCs, plastidic phosphoglucose isomerase (pPGI) acts as an important determinant of photosynthesis and growth, likely as a consequence of its involvement in the synthesis of plastidic CKs in roots. Moreover, this enzyme plays an important role in connecting the Calvin-Benson cycle with the starch biosynthetic pathway in leaves. To elucidate the mechanisms involved in the responses of plants to microbial VCs and to investigate the extent of pPGI involvement, we characterized pPGI-null *pgi1-2* Arabidopsis plants cultured in the presence or absence of VCs emitted by *Alternaria alternata*. We found that volatile emissions from this fungal phytopathogen promote growth, photosynthesis, and the accumulation of plastidic CKs in *pgi1-2* leaves. Notably, the mesophyll cells of *pgi1-2* leaves accumulated exceptionally high levels of starch following VC exposure. Proteomic analyses revealed that VCs promote global changes in the expression of proteins involved in photosynthesis, starch metabolism, and growth that can account for the observed responses in *pgi1-2* plants. The overall data show that Arabidopsis plants can respond to VCs emitted by phytopathogenic microorganisms by triggering pPGI-independent mechanisms.

It is well known that volatile compounds (VCs) emitted by beneficial rhizosphere bacteria and fungi can promote plant growth (Ryu et al., 2003; Hung et al., 2013; Kanchiswamy et al., 2015). We recently showed that this action is not only restricted to beneficial microorganisms but extends to pathogens and microbes that do not normally interact mutualistically with plants (Sánchez-López et al., 2016). When Arabidopsis (*Arabidopsis thaliana*) plants were exposed to VCs emitted by the fungal phytopathogen *Alternaria alternata*, growth promotion was accompanied by enhanced intracellular levels of plastid-type, 2-*C*-methyl-D-erythritol 4-phosphate (MEP) pathway-derived cytokinins (CKs), augmented photosynthesis, and the accumulation of exceptionally high levels of starch in leaves (Ezquer et al., 2010; Li et al., 2011; Sánchez-López et al., 2016). Furthermore, mutants with reduced CK content or sensitivity responded poorly to VCs (Sánchez-López et al., 2016). Because CKs are major determinants of growth, photosynthesis, and starch accumulation in mature leaves (Riefler et al., 2006; Werner et al., 2008; Kieber and Schaller, 2014; Bahaji et al., 2015b), we postulated that a plant's response to VCs involves CK action (Sánchez-López et al., 2016). The transcriptome changes of plants exposed to VCs emitted by phylogenetically distant microbial species, such as *A. alternata* and the beneficial plant growth-promoting rhizobacterium *Bacillus subtilis* GB03, were strikingly similar (Sánchez-López et al., 2016), indicating that plants react to microbial VCs through highly conserved regulatory mechanisms. We have proposed that VC-promoted plant growth and metabolic changes prepare the plant to host the microorganism, which, in the case of phytopathogenic microorganisms, ensures proper continuation into the pathogenic phase (Sánchez-López et al., 2016).

Phosphoglucose isomerase (PGI) catalyzes the reversible isomerization of Glc-6-P and Fru-6-P. This enzyme is involved in glycolysis and in the regeneration of Glc-6-P molecules in the oxidative pentose phosphate

pathway. In mesophyll chloroplasts of illuminated leaves, the plastidic isoform of PGI (pPGI) also plays a fundamental role in starch biosynthesis, connecting the Calvin-Benson cycle (CBC) with the starch biosynthetic pathway that encompasses plastidic phosphoglucomutase (pPGM), ADP-Glc pyrophosphorylase (AGP), and starch synthase (SS; Bahaji et al., 2014b). Recent studies have shown that the leaves of pPGI-null *pgi1-2* mutants accumulate low levels of plastidic CKs (Bahaji et al., 2015b). These plants display reduced photosynthetic capacity and slow growth phenotypes and accumulate low levels of starch in the mesophyll cells of leaves (Bahaji et al., 2015b). However, this phenotype can be reverted to the wild type by exogenous CK supplementation (Bahaji et al., 2015b). Thus, pPGI is an important determinant of photosynthesis, starch accumulation, and growth, most likely as a consequence of its involvement in the production of oxidative pentose phosphate pathway/glycolysis intermediates that are required to synthesize plastidic CKs in roots, assimilate nitrogen, and/or maintain plastid redox homeostasis (Bahaji et al., 2015b).

A. alternata emits highly reactive VCs such as sesquiterpenes (Weikl et al., 2016). These compounds are known to function as infochemicals, playing crucial roles in plant-microbe interactions (Peñuelas et al., 2014; Ditengou et al., 2015). Although there has been a considerable increase in our knowledge regarding the importance of metabolic adjustments to changing environmental conditions in recent years, little is known about the adjustments that occur in plants following exposure to microbial VCs. Thus, to obtain insights into the mechanisms involved in the *A. alternata* VC-promoted growth, photosynthesis, and accumulation of CKs and starch, and to investigate the extent to which pPGI is involved in these responses, in this work we characterized *pgi1-2* plants exposed to *A. alternata* VCs. Our findings show that Arabidopsis is capable of responding to microbial volatile emissions by triggering pPGI-independent mechanisms and raise important questions regarding the basic mechanisms of starch biosynthesis in leaves exposed to VCs.

RESULTS AND DISCUSSION

A. alternata VCs Promote Growth and the Accumulation of High Levels of Starch in Mesophyll Cells of *pgi1-2* Plants

pgi1-2 plants were cultured in the absence or continuous presence of *A. alternata* VCs for 1 week. As shown in Figure 1A, VCs promoted growth in *pgi1-2* plants to the same extent as in wild-type plants, providing evidence that *A. alternata* VCs exert a stimulatory effect on growth through pPGI-independent mechanisms.

Time-course analyses of starch content during illumination showed that *pgi1-2* and wild-type leaves accumulate starch at rates of approximately 2 and 20 nmol Glc transferred to starch min^{-1} g^{-1} fresh weight, respectively (Fig. 1B). The rate of starch accumulation in wild-type leaves after 2 h of exposure to *A. alternata* VCs increased to approximately 330 nmol Glc transferred to starch min^{-1} g^{-1} fresh weight (Fig. 1B). Consequently, leaves of wild-type plants exposed to fungal VCs for 16 h accumulated approximately 15-fold more starch than nontreated leaves. Notably, the rate of starch accumulation in *pgi1-2* leaves after 2 to 4 h of VC exposure increased to approximately 240 nmol Glc transferred to starch min^{-1} g^{-1} fresh weight (Fig. 1B). Consequently, leaves of VC-treated *pgi1-2* plants accumulated exceptionally high levels of starch after 16 h of VC exposure (approximately 8- and 85-fold higher than those of nonexposed wild-type and *pgi1-2* leaves, respectively). The starch levels in leaves of VC-treated wild-type and *pgi1-2* plants remained high during the following 7 d of treatment (data not shown).

The finding that leaves of *pgi1-2* plants treated with fungal VCs accumulate high levels of starch was an unexpected result. To confirm that what we had measured was indeed starch, we analyzed iodine-stained leaves of wild-type and *pgi1-2* plants that had been cultured in the absence or presence of *A. alternata* VCs for 16 h. Furthermore, we conducted light microscopy analyses of Toluidine Blue-stained leaves and transmission electron microscopy (TEM) analyses of leaf mesophyll cells of VC-treated wild-type and *pgi1-2* plants. As shown in Figure 2, A, B, I, and J, the iodine staining of leaves of VC-treated wild-type and *pgi1-2* plants was darker than that of nontreated leaves. The iodine staining was homogenously distributed throughout the leaf in both VC-treated wild-type and *pgi1-2* plants, indicating that starch overaccumulation occurs mainly in the mesophyll. Light microscopy analyses of sections of the stained leaves showed that, unlike wild-type leaves, *pgi1-2* mesophyll cells were poorly stained when plants were cultured in the absence of VCs (Fig. 2, C and K). In clear contrast, the mesophyll cells of VC-treated wild-type and *pgi1-2* leaves

[1] This work was supported by the Comisión Interministerial de Ciencia y Tecnología and Fondo Europeo de Desarrollo Regional, Spain (grant nos. BIO2010–18239 and BIO2013–49125–C2–1–P), by the Government of Navarra (grant no. IIM010491.RI1), by the I-Link0939 project from the Ministerio de Economía y Competitividad, by the Ministry of Education, Youth, and Sports of the Czech Republic (grant no. LO1204 from the National Program of Sustainability), by Palacky University institutional support, by predoctoral fellowships from the Spanish Ministry of Science and Innovation (to A.M.S.-L. and P.G.-G.), and by postdoctoral fellowships from the Public University of Navarra (to M.B. and G.A.).

[2] These authors contributed equally to the article.

* Address correspondence to javier.pozueta@unavarra.es.

The author responsible for distribution of materials integral to the findings presented in this article in accordance with the policy described in the Instructions for Authors (www.plantphysiol.org) is: Javier Pozueta-Romero (javier.pozueta@unavarra.es).

A.M.S.-L., A.B., N.D.D., M.B., F.J.M., E.B.-F., and J.P.-R. designed the experiments and analyzed the data; A.M.S.-L., A.B., M.B., N.D.D., F.J.M., G.A., A.R.-B., P.G.-G., K.A., J.L., J.F.H., O.N., S.C., M.C.M., R.N., and E.B.-F. performed most of the experiments; L.S., K.D., O.N., and J.P.-R. supervised the experiments; A.M.S.-L., A.B., F.J.M., and J.P.-R. wrote the article with contributions from all the authors; J.P.-R. conceived the project and research plans.

[OPEN] Articles can be viewed without a subscription.

www.plantphysiol.org/cgi/doi/10.1104/pp.16.00945

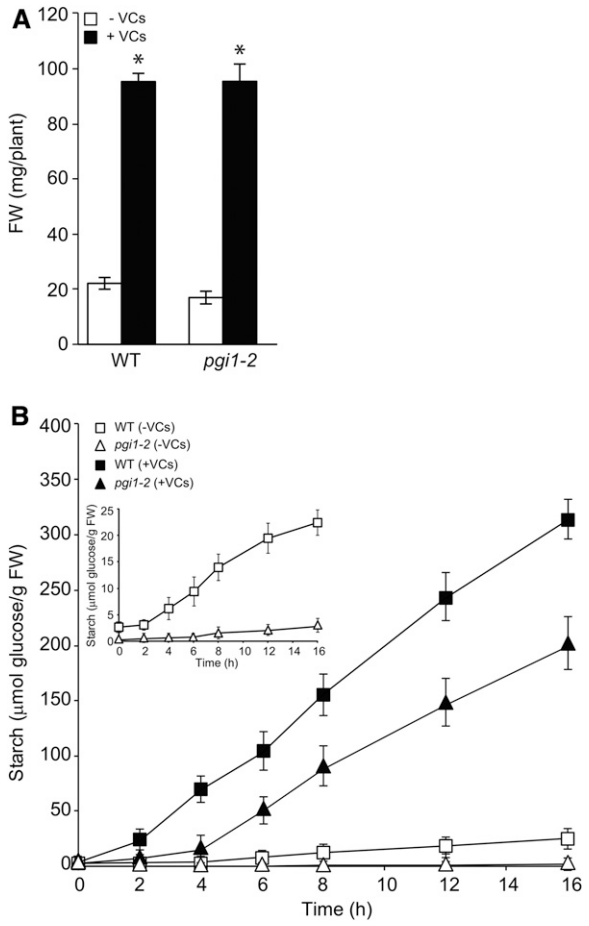

Figure 1. *A. alternata* VCs promote growth and the accumulation of exceptionally high levels of starch in the mesophyll cells of *pgi1-2* plants. Rosette fresh weight (FW; A) and time course of starch content in the leaves (B) are shown for wild-type (WT) and *pgi1-2* plants cultured in the absence or continuous presence of adjacent cultures of *A. alternata*. Values represent means ± SE determined from four independent experiments using 12 plants in each experiment. The asterisks in A indicate significant differences between microbial VC-treated plants and controls (nontreated plants) according to Student's *t* test ($P < 0.05$). The plants in A were exposed to VCs for 1 week.

were heavily stained (Fig. 2, D and L). The light microscopy (Fig. 2, E, F, M, and N) and TEM (Fig. 2, G, H, O, and P) analyses of leaves showed that the mesophyll chloroplasts of VC-treated wild-type and *pgi1-2* plants possess starch granules far larger than those of chloroplasts of plants cultured in the absence of VCs. Thus, the data show that *A. alternata* VCs stimulate important CBC-pPGI-pPGM-AGP-SS-independent starch biosynthetic pathways to allow the mesophyll cells of leaves to accumulate exceptionally high levels of starch.

A. alternata VCs Increase the Photosynthetic Activities of Exposed *pgi1-2* Plants

pPGI null mutants have a lower photosynthetic capacity than wild-type plants, which can partly explain the reduced growth and low starch content of these mutants (Bahaji et al., 2015b). We thus hypothesized that the growth promotion and accumulation of high levels of starch in *pgi1-2* plants exposed to *A. alternata* VCs could be the consequence, at least in part, of enhanced photosynthetic capacity. To test this hypothesis, we measured key parameters of the light and dark phases of photosynthesis in *pgi1-2* plants exposed to *A. alternata* VCs over 3 d. During the light phase, maximum quantum yields of PSII in the dark-adapted state (Φ_{Po}) and the PSII operating efficiency (Φ_{PSII}) were higher in leaves of the VC-treated *pgi1-2* plants than in controls (Table I), implying an improvement in the energy transfer within PSII. Furthermore, nonphotochemical quenching of chlorophyll fluorescence (Φ_{NPQ}) was reduced by exposure to VCs (Table I). These results indicate that leaves of VC-treated *pgi1-2* plants used the light more efficiently, dissipated less excitation energy as heat, had a better electron transport downstream from PSII, reduced more $NADP^+$, and, hence, had higher net rates of CO_2 assimilation (A_n) than controls. This inference was corroborated by the analyses of both photosynthetic pigments and NADPH levels as well as A_n under varying intercellular CO_2 concentrations (C_i). As shown in Figure 3A, the leaves of VC-treated *pgi1-2* plants had higher chlorophyll and carotenoid levels than in controls. Also, the NADPH content of VC-treated *pgi1-2* plant leaves (6.09 ± 0.12 nmol NADPH g^{-1} fresh weight) was higher than that of nontreated leaves (4.87 ± 0.11 nmol NADPH g^{-1} fresh weight). Moreover, *pgi1-2* plants exposed to VCs had higher A_n values than controls at all C_i levels (Fig. 3B), reaching values that were comparable to those of VC-treated wild-type plants (Sánchez-López et al., 2016). The maximum rate of carboxylation by Rubisco as well as the maximum electron transport demand for ribulose 1,5-bisphosphate regeneration determined from the A_n/C_i curves were both significantly higher in leaves of VC-treated *pgi1-2* plants than in controls, as was triose phosphate use (Table I). Furthermore, the photosynthetic electron transport rate was higher in the VC-treated *pgi1-2* plants than in controls (Fig. 3C), reaching values that were comparable to those of VC-treated wild-type plants (Sánchez-López et al., 2016). Moreover, the levels of primary photosynthates were significantly up-regulated by *A. alternata* VCs. Thus, as shown in Figure 4A, the levels of Suc, Glc, Fru, maltose, phosphorylated forms of Glc and Fru (Glc-1-P, Glc-6-P, Fru-6-P, and Fru-1,6-bisP), and CBC intermediates, such as glyceraldehyde-3-phosphate (GAP) and 3-phosphoglycerate (3PGA), were higher in the leaves of VC-treated *pgi1-2* plants than in controls. Also, total free amino acid content was higher in leaves of VC-treated plants than in controls (Fig. 4B; Supplemental Fig. S1). The most prominent free amino acids were the stress-responsive Ala as well as the high-nitrogen-containing Gln and Asn, which reflected enhanced nitrogen assimilation under VC exposure.

These results strongly indicate that *A. alternata* VCs stimulate pPGI-independent mechanisms that increase the efficiency of a plant's use of light energy

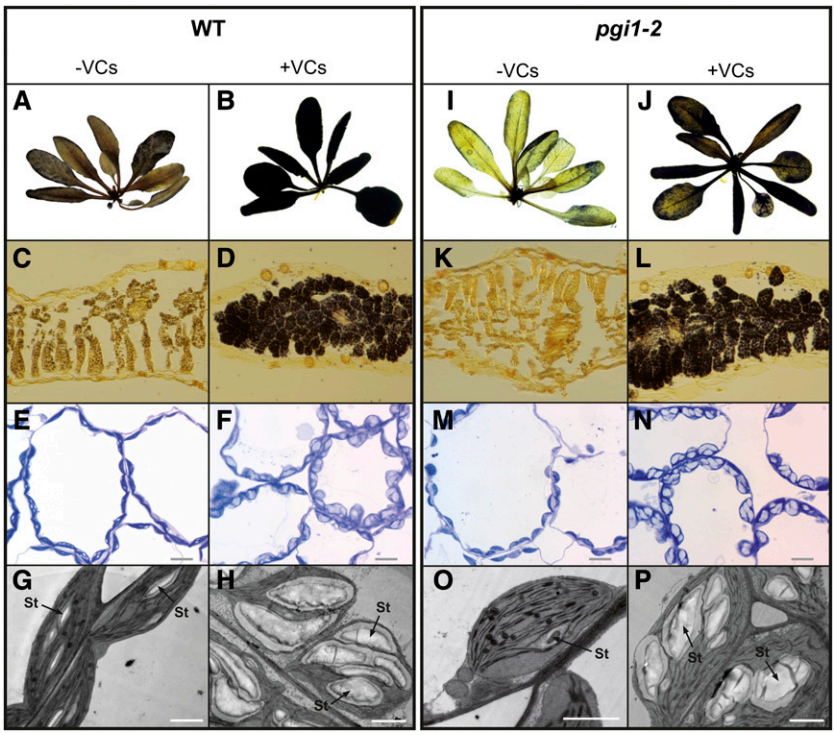

Figure 2. *A. alternata* VCs promote the accumulation of starch in mesophyll cells of *pgi1-2* leaves. A, B, I, and J, Iodine staining of whole wild-type (WT; A and B) and *pgi1-2* (I and J) plants cultured in the absence or continuous presence of VCs emitted by *A. alternata* for 14 h. C, D, K, and L, Iodine staining of cross sections of leaves of wild-type (C and D) and *pgi1-2* (K and L) plants cultured in the absence or continuous presence of VCs emitted by *A. alternata* for 14 h. E, F, M, and N, Light microscopy of the mesophyll cells of leaves of wild-type (E and F) and *pgi1-2* (M and N) plants cultured in the absence or continuous presence of VCs emitted by *A. alternata* for 14 h. Bars = 10 μm. G, H, O, and P, Electron microscopy of the mesophyll cells of leaves of wild-type (G and H) and *pgi1-2* (O and P) plants cultured in the absence or continuous presence of VCs emitted by *A. alternata* for 14 h. St, Starch. Bars = 2 μm.

in photosynthesis and enhance the formation of photosynthates.

A. alternata VCs Promote the Accumulation of Active Forms of Plastidic CKs in *pgi1-2* Leaves

Plastidic MEP pathway-derived CKs are synthesized mainly in roots and transported to the aerial parts of the plant, where they regulate plant growth (Ko et al., 2014). We recently provided evidence that pPGI is an important determinant of plastidic CK content in leaves, and this is most likely based on its involvement in the synthesis of GAP (Bahaji et al., 2015b), the substrate for the initial reaction of the plastidic MEP pathway (Pulido et al., 2012; Pokhilko et al., 2015). To investigate the possible involvement of pPGI in the VC-promoted increase of plastidic CKs in wild-type leaves (Sánchez-López et al., 2016), we measured the levels of different CKs in the leaves of *pgi1-2* plants that had been cultured in the absence or presence of VCs emitted by *A. alternata* for 3 d. As shown in Table II, exposure to VCs caused a significant increase of the total content of MEP-derived CKs in *pgi1-2* leaves. The total content of MEP-derived CKs in VC-treated *pgi1-2* leaves (1,193.24 ± 100.89 pmol g^{-1} dry weight; Table II) was lower than that of VC-treated wild-type leaves (1,534.78 ± 23.61 pmol g^{-1} dry weight; compare with Table 2 in Sánchez-López et al., 2016). Moreover, the VC-promoted augmentation of total CK content in *pgi1-2* leaves (approximately 400 pmol g^{-1} dry weight; Table II) was comparable to what had been observed in wild-type leaves (compare with Table 2 in Sánchez-López et al., 2016), indicating that pPGI plays only a minor role in the VC-promoted accumulation of CKs in wild-type leaves. The most prominent CK forms were the biologically active isopentenyladenine (iP) and trans-zeatin (tZ) as well as their ribosides (iPR and tZR, respectively) and precursors (iPRMP and tZRMP, respectively). On the other hand, the levels of the less biologically active CKs dihydrozeatin (DZ) and cis-zeatin (cZ) were reduced substantially (Table II; Supplemental Fig. S2).

As for the pPGI-independent mechanisms that may have contributed to the increase in MEP-derived CKs in the leaves of VC-treated *pgi1-2* plants, it should be noted

Table I. *Photosynthetic parameters of the leaves of pgi1-2 plants cultured in the absence or presence of VCs emitted by A. alternata for 3 d*
Values represent means ± SE of determinations from four independent experiments.

Treatment	Φ_{Po}	Φ_{PSII}	Φ_{NPQ}	Maximum Electron Transport Demand for Ribulose 1,5-Bisphosphate Regeneration	Maximum Rate of Carboxylation by Rubisco	Triose Phosphate Use
				$\mu mol\ e^{-}\ m^{-2}\ s^{-1}$	$\mu mol\ CO_2\ m^{-2}\ s^{-1}$	μmol inorganic phosphate $m^{-2}\ s^{-1}$
− VCs	0.69 ± 0.01	0.35 ± 0.01	0.89 ± 0.04	25.3 ± 0.33	15.5 ± 0.42	1.08 ± 0.06
+ VCs	0.82 ± 0.01	0.48 ± 0.01	0.35 ± 0.03	59.0 ± 0.46	25.3 ± 0.26	2.89 ± 0.09

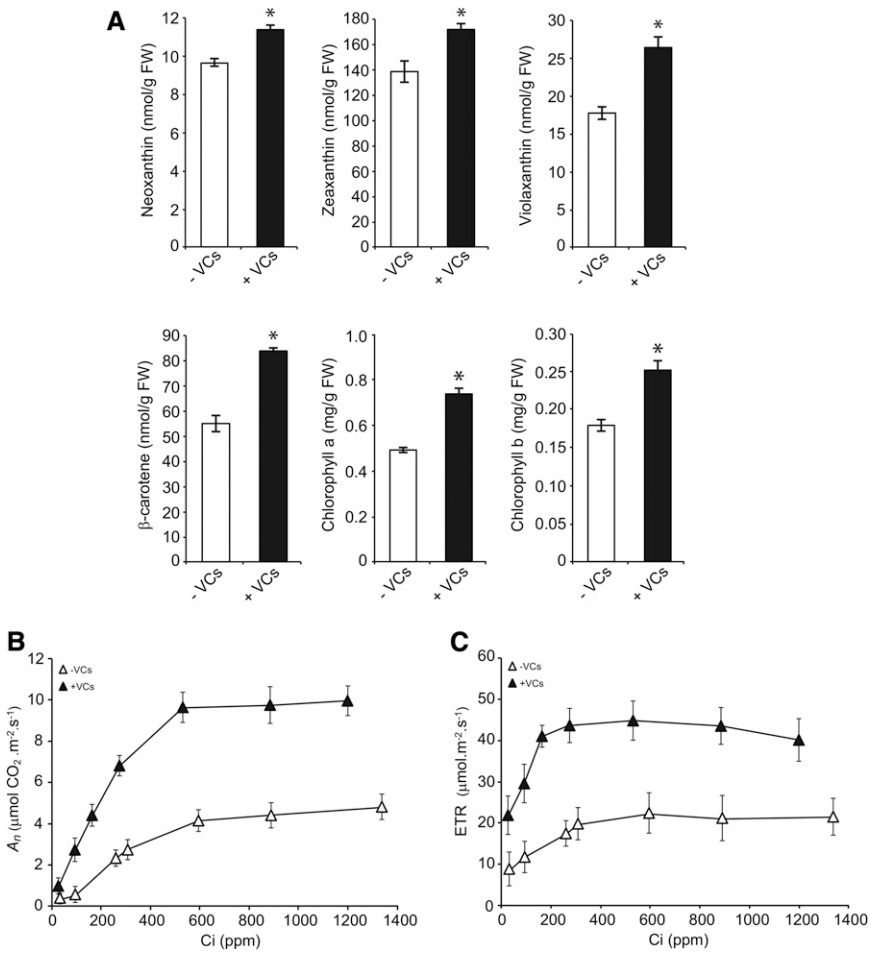

Figure 3. *A. alternata* VCs enhance photosynthesis in the leaves of *pgi1-2* plants. Levels of photosynthetic pigments (A), A_n curves (B), and photosynthetic electron transport rate (ETR) versus C_i (C) are shown in leaves of *pgi1-2* plants cultured in the absence or continuous presence of adjacent cultures of *A. alternata* for 3 d. Treatment with VCs started at 18 d after the sowing growth stage of plants. Values in A represent means ± SE determined from four independent experiments using 12 plants in each experiment. Asterisks indicate significant differences between the leaves of VC-treated and control (nontreated) plants according to Student's *t* test ($P < 0.05$). FW, Fresh weight.

that the GAP content in VC-treated *pgi1-2* leaves was 2-fold higher than that of nontreated leaves (Fig. 4A), likely as a consequence of enhanced photosynthesis. Therefore, the accumulation of high levels of MEP-derived CKs in the leaves of VC-treated *pgi1-2* plants may be partly due to the enhanced photosynthetic production of GAP and its subsequent conversion to MEP-derived CKs (Supplemental Fig. S2). Another mechanism that could explain the pPGI-independent enhancement of plastidic CKs in VC-treated leaves is the conversion of cytosolic GAP into isopentenyl diphosphate and/or dimethylallyl diphosphate (DMAPP) and the subsequent transport of these metabolites into the chloroplast, which could increase the DMAPP pool available for plastid-localized isopentenyltransferases (Supplemental Fig. S2). This mechanism of isopentenyl diphosphate and/or DMAPP exchange between the cytosol and plastids has been proposed as the MVA-derived contribution to plastidic biosynthesis of GAs (Helliwell et al., 2001).

Regarding the mechanism(s) that may be involved in the VC-promoted increase in the active and transport forms of MEP-derived CKs and their precursors in *pgi1-2* leaves, it should be noted that levels of the less biologically active CKs cZ, cZR, and DZ, and levels of the *N*- and *O*-glycosylated inactive forms DZOG, DZ7G, cZOG, and cZ9G, were lower than in controls (Table II; Supplemental Fig. S2). This indicates that the down-regulation of enzymes involved in the conversion of tZ into DZ, as well as in the degradation of active plastidic CKs, could play a role in the VC-promoted accumulation of active and transport forms of MEP-derived CKs and their precursors.

A. alternata VCs Promote Changes in the Proteome of *pgi1-2* Leaves That Account for the Observed Physiochemical Responses

The results presented above show that *A. alternata* VCs stimulate important pPGI-independent mechanisms, resulting in the enhancement of photosynthesis, growth, and starch overaccumulation in leaves. To obtain insights into these mechanisms, we carried out high-throughput, isobaric labeling-based differential proteomic and phosphoproteomic analyses of leaves from *pgi1-2* plants cultured in the absence or in the presence of VCs emitted by *A. alternata* for 3 d. As shown in Supplemental Table S1, these analyses revealed that, in the presence of *A. alternata* VCs, 226 out of the 3,805 proteins identified in this study (Supplemental Table S2) were up-regulated and 60 proteins were down-regulated. Using the broad characterizations outlined by MapMan, the 286 proteins that were differentially regulated by *A. alternata* VCs were

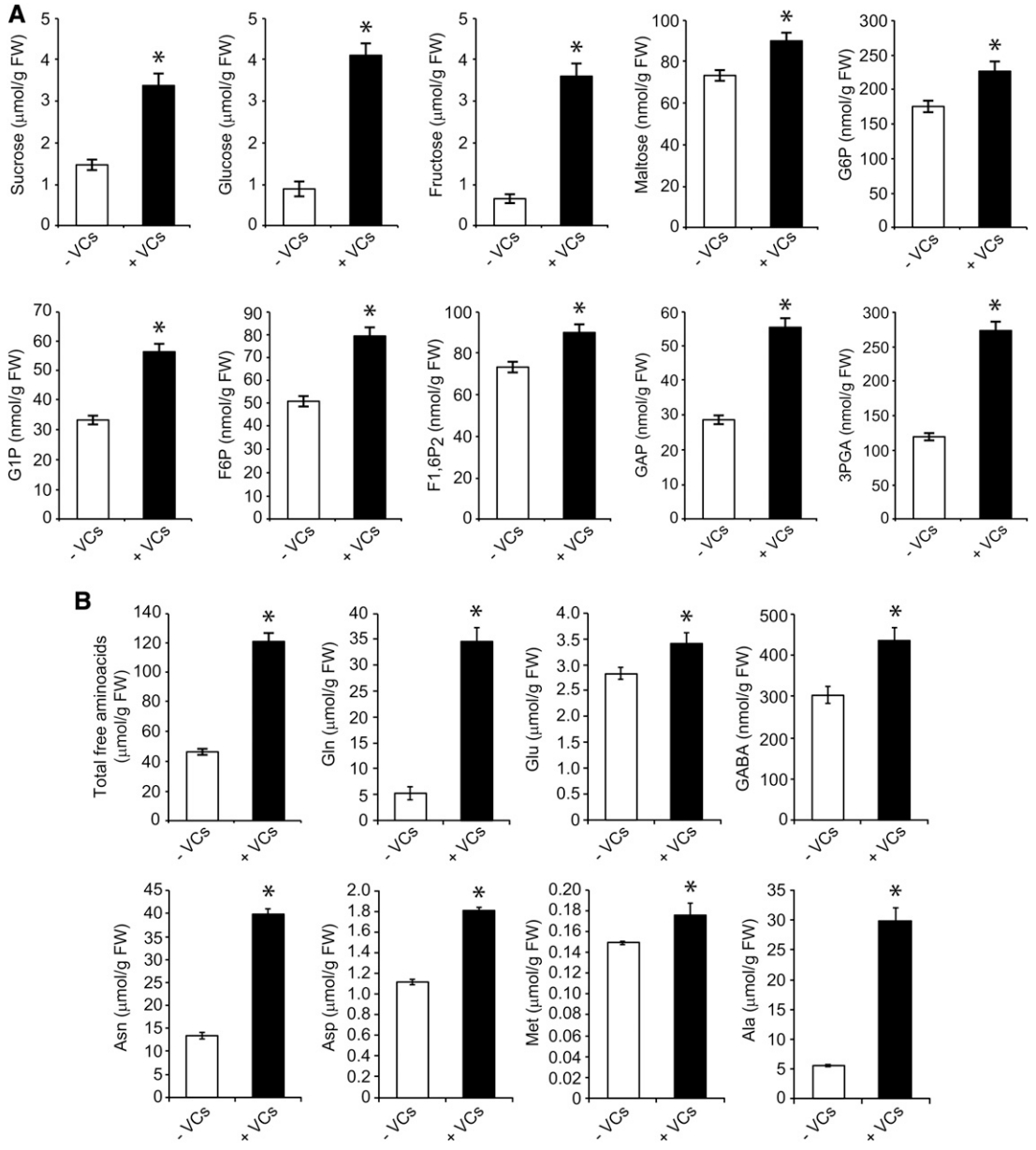

Figure 4. *A. alternata* VCs increase photosynthate levels in *pgi1-2* leaves. Carbohydrate contents (A) and free amino acid contents (B) are shown in leaves of plants grown in the absence or continuous presence of adjacent cultures of *A. alternata* for 3 d. Leaves were harvested at the end of the light period. Values represent means ± SE determined from four independent experiments using 12 plants in each experiment. Asterisks indicate significant differences between the leaves of VC-treated and control (nontreated) plants according to Student's *t* test ($P < 0.05$). FW, Fresh weight.

assembled into 29 functional groups (Fig. 5). These proteins also were classified into eight groups according to their subcellular localizations, and the chloroplastic proteins were shown to be the most differentially regulated (Supplemental Table S3; Supplemental Fig. S3). Nearly 9% of the proteins of *pgi1-2* leaves differentially regulated by VCs are encoded by CK-responsive genes (Supplemental Table S1; Fig. 5), which reinforces the idea that CKs play an important role in the response of plants to *A. alternata* VCs (Sánchez-López et al., 2016). Moreover, 21% of the proteins that where differentially regulated by VCs are encoded by genes whose expression also was differentially regulated by *A. alternata* VCs (Sánchez-López et al., 2016; Supplemental Table S1), indicating that VC-promoted changes in the proteome of *pgi1-2* leaves are subject to both transcriptional and posttranscriptional regulation. The general trend indicates that VC-promoted responses are the consequence, at least partly, of changes in the expression of proteins from the following groups: photosynthesis, protection against photoinhibition and

Table II. *CK contents (pmol g^{-1} dry weight) in leaves of pgi1-2 plants that were, at 18 d after sowing, cultured in solid MS medium in the absence or presence of VCs emitted by A. alternata for 3 d*

CK precursors, transport forms, active forms, and glycosylated inactive forms are separated into two groups based on their origin from either the MEP or mevalonate (MVA) pathway. Total sums and corresponding percentage are shown for individual forms. Asterisks indicate significant differences according to ANOVA: *, $P < 0.05$; **, $P < 0.01$; and ***, $P < 0.001$.

Sample	MEP Pathway (Plastid)-Derived CKs			MVA Pathway (Cytosol)-Derived CKs		
	Name	*pgi1-2* − VCs	*pgi1-2* + VCs	Name	*pgi1-2* − VCs	*pgi1-2* + VCs
Precursors	iPRMP	171.05 ± 21.87	392.91 ± 20.91***			
	tZRMP	129.90 ± 18.80	266.38 ± 53.22**	cZRMP	116.38 ± 13.30	141.51 ± 3.49*
	DZRMP	2.51 ± 0.30	1.23 ± 0.11**			
	∑ (%)	303.46 ± 28.77	660.53 ± 52.33**		116.38 ± 13.30	141.51 ± 3.49*
Transport forms	iPR	12.58 ± 2.07	18.74 ± 2.03*			
	tZR	10.56 ± 0.93	23.32 ± 2.40**	cZR	11.03 ± 0.61	5.46 ± 0.29***
	DZR	0.56 ± 0.03	0.17 ± 0.02***			
	∑ (%)	23.71 ± 0.84	42.23 ± 1.44***		11.03 ± 0.61	5.46 ± 0.29***
Active forms	iP	3.66 ± 0.20	5.92 ± 0.25***			
	tZ	6.49 ± 0.27	9.16 ± 1.55*	cZ	2.98 ± 0.09	1.73 ± 0.16***
	DZ	0.36 ± 0.02	0.02 ± 0.01***			
	∑ (%)	10.51 ± 0.25	15.10 ± 1.27*		2.98 ± 0.09	1.73 ± 0.16***
Glycosylated (inactive) forms	iP7G	86.25 ± 4.53	80.78 ± 8.79			
	tZ7G	112.54 ± 1.04	109.09 ± 7.70			
	DZ7G	33.35 ± 0.89	20.12 ± 2.77**			
	iP9G	14.83 ± 0.83	14.76 ± 0.95	cZ9G	4.22 ± 0.35	2.68 ± 0.63*
	tZ9G	133.17 ± 15.21	176.02 ± 45.30			
	DZ9G	2.01 ± 0.51	1.17 ± 0.37			
	tZOG	40.87 ± 0.92	38.76 ± 1.59	cZOG	17.18 ± 0.62	10.16 ± 0.92***
	DZOG	6.37 ± 1.49	3.89 ± 0.80			
	tZROG	27.45 ± 4.40	27.12 ± 8.35	cZROG	47.71 ± 12.60	40.01 ± 7.19
	DZROG	5.50 ± 1.19	3.67 ± 0.62			
	∑ (%)	462.55 ± 9.76	475.38 ± 47.36		69.11 ± 9.57	52.84 ± 5.36
Total	∑ (%)	800.24 ± 24.59	1,193.24 ± 100.89*		199.50 ± 14.15	201.53 ± 8.02

photooxidative damage, cell wall biosynthesis, as well as amino acid and central carbohydrate metabolism.

Photosynthesis

VCs promoted the expression of proteins that participate directly in the synthesis of chlorophyll (e.g. PORB, PORC, PCB2, CHLH, CRD1, CHLI1, and GUN4; Supplemental Table S1; Fig. 5), which is consistent with the enhanced chlorophyll content observed in the leaves of VC-treated plants (Fig. 3A). Exposure to VCs also up-regulated the expression of enzymes involved in the conversion of SO_4^{2-} into SO_3^{2-} (e.g. the CK up-regulated APR2, APR3, APS1, and APS3; Supplemental Table S1; Fig. 5) and the conversion of SO_3^{2-} into sulfoquinovosyldiacylglycerol (SQD1 and SQD2), a sulfolipid that acts as an integral component of the PSII protein complex and helps maintain the negatively charged lipid-water interface required for the proper functioning of photosynthetic membranes (Frentzen, 2004). VC treatment also increased the expression of the PSII reaction center proteins PsbT and PsbH (Supplemental Table S1; Fig. 5). Notably, phosphoproteomic analyses revealed that VCs promoted changes in the phosphorylation status of PsbH and LHCB4.1 (Supplemental Table S1). The phosphorylation of PSII proteins is required for the adequate lateral mobility of membrane proteins, sustained photosynthetic activity, and to prevent oxidative damage of photosynthetic proteins (Fristedt et al., 2009). The data presented thus indicate that VC-promoted enhancement of photosynthesis in *pgi1-2* plants is the result of enhanced enzymatic production of chlorophyll and sulfoquinovosyldiacylglycerol along with the up-regulation of, and changes in the phosphorylation status, of PSII proteins (Fig. 6).

Protection against Photoinhibition and Photooxidative Damage

The *A. alternata* VC-promoted increase of electron transport rate (Fig. 3C) could create conditions under which reactive oxygen species (ROS) are produced. Therefore, it is conceivable that VCs would trigger mechanisms that prevent ROS production and/or photooxidative damage, allowing the plant to convert more light into chemical energy under VC exposure. In line with this presumption, we found that VCs positively influence the expression of enzymatic ROS scavengers (e.g. MSBP2, APX1, CAT3 and AHB2) as well as proteins that prevent the formation of ROS (e.g. FER1 and FER3; Supplemental Table S1; Fig. 5). Some of these proteins (e.g. AHB2) have been shown to be transcriptionally up-regulated by CKs and to act as important determinants of growth (Hunt et al., 2001, 2002).

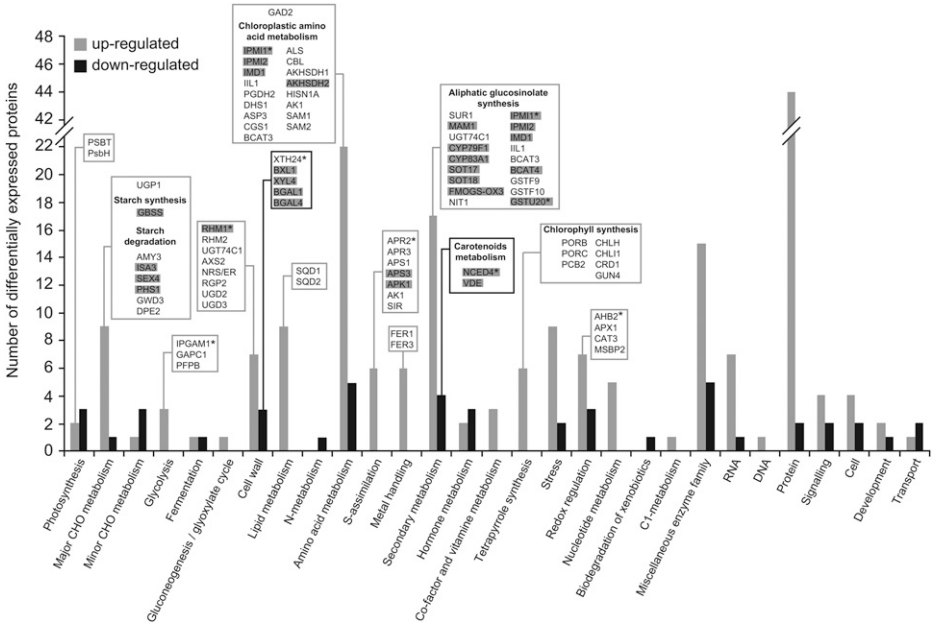

Figure 5. Functional categorization of the differentially expressed proteins in leaves of *pgi1-2* plants cultured in the presence of VCs emitted by *A. alternata*. Proteins that were both significantly down- and up-regulated following VC exposure were sorted according to the putative functional category assigned by MapMan software. The number of up- and down-regulated proteins in each categorical group is indicated by gray and black bars, respectively. Proteins discussed here are boxed. Proteins encoded by genes that are differentially expressed in the leaves of VC-treated plants are indicated in gray, and CK-regulated proteins are indicated with asterisks.

Consistent with the increased content of carotenoids observed in VC-treated *pgi1-2* leaves (Fig. 3A), VCs exerted a negative effect on the expression of NCED4 (Supplemental Table S1; Fig. 5), a protein that is involved in carotenoid degradation and transcriptionally down-regulated by CKs (Gonzalez-Jorge et al., 2013). An essential role of carotenoids in photosynthesis is the protection against photooxidative damage (Ruiz-Sola and Rodríguez-Concepción, 2012), and in this way, NCED4 down-regulation may contribute to the enhanced photosynthetic capacity observed in VC-treated plants (Fig. 5; Table I).

Cell Wall Biosynthesis

Since cell wall composition and extensibility are major determinants of growth, it is conceivable that the VC-promoted growth of *pgi1-2* plants partly involved changes in the expression of cell wall-related enzymes. The proteomic analysis provided evidence for this hypothesis, as it revealed that VC exposure altered the expression of a number of enzymes that participate in cell wall composition and extensibility (e.g. RHM1, RHM2, UGT74C1, AXS2, NRS/ER, RGP2, UGD2, UGD3, XTH24, BXL1, XYL4, BGAL1, and BGAL4; Supplemental Table S1; Fig. 5). Some of these enzymes (e.g. RHM1 and XTH24) are regulated by CKs.

Amino Acid Metabolism

VCs positively affected the expression of enzymes that are involved in the conversion of 3PGA from the CBC and plastidic Gln into Met (e.g. the chloroplastic PGDH2, ASP3, AKHSDH1, AKHSDH2, CGS1, and CBL; Supplemental Table S1; Fig. 5) as well as the conversion of Glu into Ala through the GABA shunt (e.g. GAD2), which would explain the accumulation of high levels of Ala, GABA, Glu, Asp, Asn, and Met observed in VC-treated leaves (Figs. 4B and 6).

VCs also up-regulated the expression of enzymes involved in the conversion of Met and Cys into aliphatic glucosinolates, including those involved in chain elongation reactions (e.g. BCAT3, BCAT4, IPMI1, IPMI2, IMD1, and MAM1), the construction of the glucosinolate core (e.g. APK1, CYP79F1, CYP83A1, GSTU20, SUR1, UGT74C1, SOT17, and SOT18), and secondary modifications (e.g. FMOGS-OX3; Supplemental Table S1; Fig. 5). Glucosinolates are sulfur-rich, amino acid-derived secondary metabolites that act as important determinants of plant growth, development, and defense against pathogens (Tantikanjana et al., 2001; Sønderby et al., 2010; He et al., 2011; Imhof et al., 2014). Some of the differentially regulated enzymes involved in glucosinolate biosynthesis (e.g. IPMI1 and GSTU20) are up-regulated by CKs (Brenner and Schmülling, 2015). Others (e.g. CYP79F1) play important roles in modulating the intracellular levels of CKs (Tantikanjana et al., 2004). Thus, it is likely that the VC-promoted up-regulation of enzymes involved in glucosinolate biosynthesis contributed to the enhanced growth of *pgi1-2* plants.

Central Carbohydrate Metabolism

VCs positively affected the expression of granule-bound SS (Supplemental Table S1; Fig. 5). Moreover, VCs up-regulated the expression of a number of starch breakdown enzymes (e.g. AMY3, ISA3, SEX4, PHS1, and GWD3; Supplemental Table S1; Fig. 5), which is

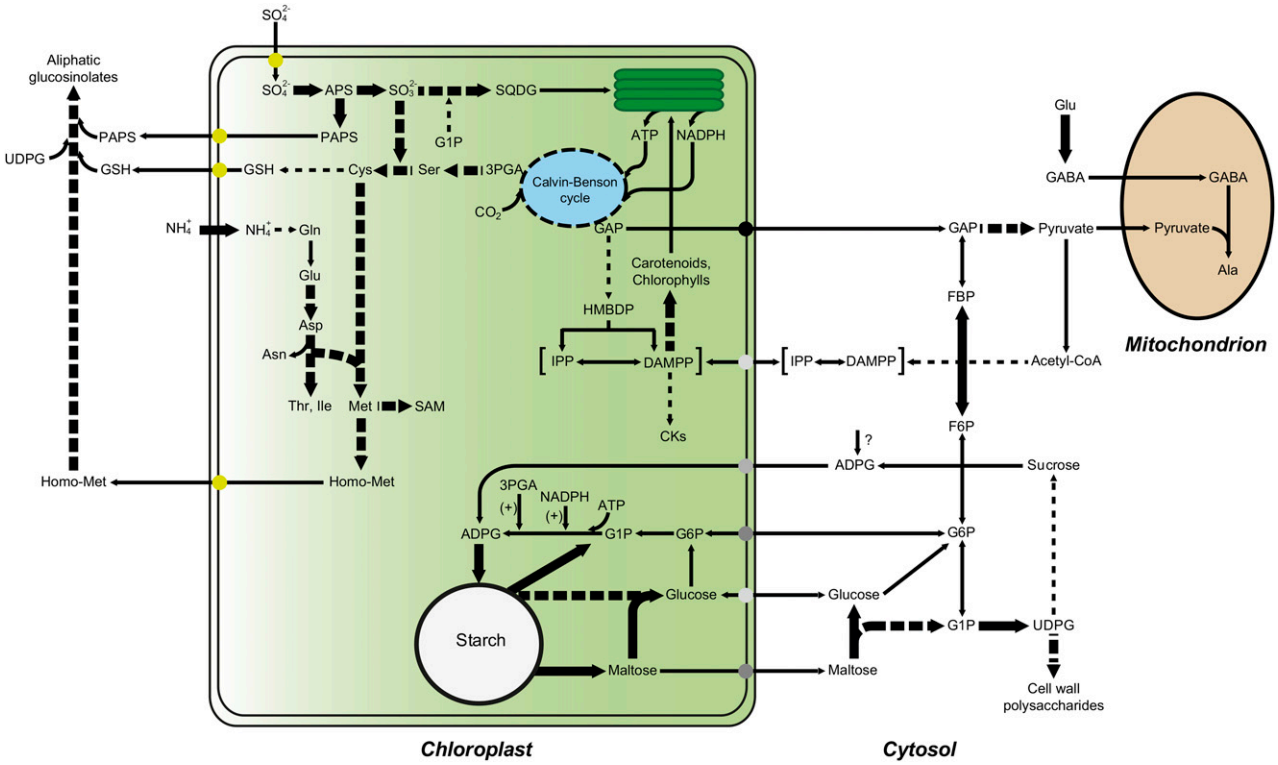

Figure 6. Scheme illustrating the metabolic adjustment that occurs in leaves of *pgi1-2* plants in response to *A. alternata* VC exposure. The VC-promoted up-regulation of PSII reaction center proteins and enzymes involved in the synthesis of sulfolipid and photosynthetic pigments results in enhanced photosynthetic activity. The resulting augmentation of GAP fuels the production of MEP-derived compounds, such as photosynthetic pigments and plastidic CKs, which initiate a cascade of reactions that cause various responses, such as the production of proteins involved in photoprotection, cell wall production and modification, and amino acid biosynthesis (Sánchez-López et al., 2016). Gln is metabolized to Glu, Asp, Asn, Met, and aliphatic glucosinolates. Also, cytosolic Glu is metabolized to Ala through the γ-aminobutyrate (GABA) shunt. According to this model, VC-promoted starch overaccumulation in *pgi1-2* leaves is the consequence of the stimulation of starch biosynthetic pathways that bypass pPGI through the transport of cytosolic hexoses (e.g. Glc and/or Glc-6-P) and/or ADP-Glc (ADPG) into the chloroplast. The high levels of 3PGA and NADPH resulting from VC-enhanced photosynthesis activate AGP (Li et al., 2011), which, in turn, facilitates the synthesis of starch. VCs also increase the expression of starch breakdown enzymes to prevent the excessive accumulation of starch and establish a starch substrate cycle. Starch breakdown products can be exported to the cytosol for their subsequent conversion into UDP-Glc, which is necessary for the synthesis of Suc and/or cell wall polysaccharides. Enzymes that are up-regulated by VCs are indicated with thick arrows. Multistep reactions are depicted with dashed arrows.

consistent with the occurrence of high levels of maltose observed in VC-treated leaves (Fig. 4). The up-regulation of starch breakdown enzymes may reflect a mechanism that aims to prevent the excessive accumulation of starch and points to the possible stimulation by VCs of starch degradation and the cycling of starch breakdown products during illumination. The resulting futile cycle (Fig. 6) may entail advantages such as buffering of metabolite levels, improved sensitivity in metabolic regulation, and the rapid channeling of metabolites to various pathways in response to the physiological and biochemical needs imposed by VC exposure. For example, Glc-1-P derived from starch breakdown could be utilized to produce sulfolipids, which, as discussed above, could result in enhanced photosynthesis. Also, hexose phosphates derived from starch breakdown could supply carbon to the CBC, a phenomenon that occurs when plants are cultured under photorespiratory conditions (Weise et al., 2006). Furthermore, maltose derived from starch degradation could act as a protectant of proteins, membranes, and the photosynthetic electron transport chain (Kaplan and Guy, 2004). On the other hand, the maltose could be exported to the cytosol for conversion into the UDP-Glc necessary for the synthesis of Suc and/or cell wall polysaccharides (Fig. 6). In support of the latter hypothesis, we found that VCs positively affect the expression of enzymes involved in the starch-to-Suc conversion process (e.g. UGP1 and DPE2).

CONCLUSION

In Arabidopsis plants not exposed to VCs, pPGI acts as an important determinant of photosynthesis, starch accumulation, and growth partly as a consequence of its involvement in the production of plastidic CKs in

roots (Bahaji et al., 2015b). In this work, we have shown that the promotion of photosynthesis, growth, and starch overaccumulation by VCs involves the stimulation of pPGI-independent mechanisms partly as a consequence of the photosynthesis-driven enhancement of plastidic CK production in leaves, which, in turn, further promotes photosynthesis (Fig. 6). This phenomenon is accompanied by the accumulation of stress-responsive amino acids such as Ala and GABA (Fig. 4B), which may represent a strategy for adaptation to the environmental conditions caused by exposure to VCs emitted by *A. alternata*. The finding that leaves of *pgi1-2* plants exposed to fungal VCs accumulate exceptionally high levels of starch (Figs. 1 and 2) when the rate of photosynthesis increases (Fig. 3) conflicts with the widely accepted view that the whole photosynthesis-driven starch biosynthetic process occurs solely in the chloroplast by means of the CBC-pPGI-pPGM-AGP-SS pathway. On the other hand, this finding is consistent with the idea that the starch deficiency in *pgi1-2* leaves not exposed to VCs is partly due to the reduced CO_2 fixation capacity of this mutant, rather than only a consequence of the lack of pPGI-mediated flow between the CBC and the pPGM-AGP-SS starch biosynthetic pathways (Bahaji et al., 2015b).

Taken together, the results presented here indicate that VC-promoted starch overaccumulation in the mesophyll cells of *pgi1-2* leaves is the consequence of factors such as enhanced photosynthesis (Fig. 3), the allosteric and redox activation of AGP by enhanced levels of photosynthetically produced 3PGA and NADPH (Li et al., 2011), the up-regulation of granule-bound SS expression (Supplemental Table S1; Fig. 5), and the stimulation of incorporation into the chloroplast of cytosolic hexoses that, once there, are converted into starch (Fig. 6). Regarding the mechanism(s) of uptake of cytosolic hexoses linked to starch biosynthesis within mesophyll chloroplasts of *pgi1-2* leaves, it should be noted that Arabidopsis contains two functional plastidic Glc-6-P/inorganic phosphate translocators (GPT1 and GPT2) that are capable of transporting hexose phosphates (Kammerer et al., 1998). Although the chloroplasts of mature wild-type leaves are not capable of transporting hexose phosphates (Quick et al., 1995; Kunz et al., 2010), most likely as a consequence of the marginally low expression of *GPT1* and *GPT2* (Kammerer et al., 1998), *GPT2* has been shown to be expressed in *pgi1-2* leaves (Kunz et al., 2010). Therefore, it is likely that starch biosynthesis occurring in the mesophyll cells of VC-treated *pgi1-2* leaves involves the GPT2-mediated transport of cytosolic Glc-6-P into the chloroplast (Fig. 6). Chloroplasts possess both a Glc transporter (pGlcT; Weber et al., 2000) and hexokinase (Giese et al., 2005), which potentially enable the incorporation of cytosolic Glc and its subsequent conversion into Glc-6-P, facilitating the bypass of the pPGI step in *pgi1-2* leaves (Fig. 6). However, pGlcT has been shown to export the Glc arising from starch breakdown to the cytosol during the night rather than to import cytosolic Glc to the chloroplast (Weber et al., 2000; Cho et al., 2011). Chloroplasts from mature leaves also possess a yet to be identified ADPG transport machinery (Pozueta-Romero et al., 1991). Taking into account that a sizable pool of ADPG linked to starch biosynthesis has a cytosolic localization in leaves (Baroja-Fernández et al., 2004; Bahaji et al., 2011, 2014a), it is likely that the starch biosynthesis observed in the mesophyll cells of VC-treated mature leaves partly involves the cytosolic production of ADPG, its subsequent transport into the chloroplast, and, then, conversion into starch (Fig. 6). Needless to say, further research will be necessary to identify the cytosolic hexose molecules that enter the chloroplast in VC-treated leaves for their subsequent conversion into starch.

MATERIALS AND METHODS

Plant and Microbial Cultures, Growth Conditions, and Sampling

The experiments were carried out using Arabidopsis (*Arabidopsis thaliana*) ecotype Wasilewskija-2 (Nottingham Arabidopsis Stock Centre; N1601) and the *pgi1-2* T-DNA insertion mutant (Kunz et al., 2010). Plants were cultured in petri dishes containing Suc-free solid Murashige and Skoog (MS) medium (Duchefa Biochemie; catalog no. M0222) in growth chambers with a 16-h-light/8-h-dark photoperiod (80 μmol photons s^{-1} m^{-2}, 22°C during the light period and 18°C during the dark period). *Alternaria alternata* was cultured in petri dishes containing solid MS medium supplemented with 90 mM Suc. Unless indicated otherwise, the effect of *A. alternata* VCs on plants was investigated by placing microbial cultures without lids and plant cultures (14 d after sowing) into sterile plastic boxes (IT200N Instrument Try 200 × 150 × 50 mm; AWGregory) and sealed with a plastic film (for details, see Sánchez-López et al., 2016). Leaves were harvested for characterization at specified incubation periods. As a negative control, petri dishes containing fully developed plants were cultured in sealed plastic boxes together with petri dishes containing sterile microbial culture medium. Harvested leaves were immediately freeze clamped and ground to a fine powder in liquid nitrogen with a pestle and mortar.

Determination of Gas-Exchange Rates and Photosynthetic Parameters

The determination of gas-exchange rates and the calculation of photosynthetic parameters were conducted as described by Sánchez-López et al. (2016) using the LI-COR 6400 gas-exchange portable photosynthesis system (LI-COR). Chlorophyll fluorescence emission parameters were determined using the PlantScreen XYZ System (Photon Systems Instruments). The phenotyping system was equipped with a FluorCam unit for pulse amplitude-modulated measurement of chlorophyll fluorescence. After 20 min of dark adaptation, the standardized measurement protocol was applied, as described by Humplík et al. (2015). The parameters Φ_{Po}, Φ_{PSII}, and Φ_{NPQ} were calculated from the measured parameters according to Lazár (2015).

Analytical Procedures

Soluble sugars were measured as described by Bahaji et al. (2015a). GAP and 3PGA were measured as described by Vogt et al. (1998) and Lytovchenko et al. (2002), respectively. The amino acid contents were determined as described by Loiret et al. (2009). Recovery experiments were carried out by adding known amounts of metabolite standards to the frozen tissue slurry immediately after the addition of extraction solutions. The difference between the measurements from samples with and without added standards was used as an estimate of the percentage of recovery. All data were corrected for losses during extraction.

Chlorophyll and carotenoid contents were quantified according to Lichtenthaler (1987) and Gonzalez-Jorge et al. (2013), respectively. Starch was measured with an amyloglucosidase-based test kit (Boehringer Mannheim). To determine the levels of CKs, aliquots of the frozen leaves (see above) from *pgi1-2* plants were lyophilized, and CKs were quantified according to the method described by Novák et al. (2008).

Iodine Staining and Microscopic Localization of Starch Granules

Experiments were conducted essentially as described by Ovecka et al. (2012). Leaves harvested at the end of the light period were fixed by immersion into 3.7% formaldehyde in phosphate buffer. Leaf pigments were then removed in 96% ethanol. Rehydrated samples were stained in an iodine solution (2% [w/v] KI and 1% [w/v] I_2) for 30 min, rinsed briefly in deionized water, and photographed. Samples for sectioning were immersed in cryoprotective medium OCT (Tissue-Tec) and frozen at −50°C. A Thermo Shandon AS620 Cryotome was used to obtain 10-μm-thick cryosections. After thawing, the sections were stained in iodine solution for 2 min at room temperature, mounted on microscope slides, and observed using an Olympus MVX10 stereomicroscope. Microphotographs were captured with a DP72 video camera (Olympus) and Cell D software (Olympus).

Light Microscopy and TEM

Small pieces (2 mm^2) of leaves were immediately fixed by submersion in a 3% (v/v) glutaraldehyde solution buffered by 0.05 M sodium cacodylate buffer, pH 7.4 (3 h at 4°C, under vacuum). After fixing, the specimens were washed in a cacodylate buffer (0.05 M sodium cacodylate and 1% Suc), three times for 30 min each at 4°C, and postfixed overnight at 4°C with a solution of 1% osmium tetroxide in the cacodylate buffer specified above. After two washes, 30 min each, at 4°C in the same cacodylate buffer, the samples were dehydrated in an ethanol series and progressively embedded in LR White resin (London Resin). Ultrathin (70–90 nm) sections for TEM were contrasted with 2% aqueous uranyl acetate and lead citrate. Observations were performed with a STEM LEO 910 electron microscope (Carl Zeiss) equipped with a Gatan Bioscan 792 camera (Gatan) at 80 kV. Semithin (1 μm) sections for light microscopy were stained with 1% (w/v) Toluidine Blue in aqueous 1% sodium borate prior to direct observation with a Zeiss Axiophot photomicroscope (Carl Zeiss).

Proteomic Analysis

Protein Sample Preparation

Samples were prepared by grinding 200 mg of leaf material into a fine powder under liquid nitrogen using a precooled mortar and pestle. The powder was then mixed with 400 μL of cold protein extraction buffer [150 mM Tris-HCl (pH 8), 6 M urea, 2% (w/v) SDS, 5% (v/v) glycerol, 5 mM Tris(2-carboxyethyl) phosphine, 2% protease inhibitor cocktail 3 (Sigma-Aldrich; catalog no. P0044), and 2% protease inhibitor cocktail (Sigma-Aldrich; catalog no. P9599)]. After 5 min at 95°C, the mixture was centrifuged at 14,000*g* for 10 min at 4°C.

Enzymatic Digestion and TMT-6 Plex Labeling

Proteins (80 μg) from the supernatant were precipitated by the methanol/chloroform method (Fic et al., 2010), after which they were denatured in 7 M urea/2 M thiourea/100 mM TEAB (pH 7.5) and reduced with 50 mM Tris(2-carboxyethyl) phosphine (pH 8) for 60 min at 37°C. Cys residues were then alkylated with 200 mM methyl methanethiosulfonate (Pierce MMTS; Thermo Fisher Scientific) for 10 min at room temperature. The urea/thiourea concentration was adjusted to 2 M in TEAB prior to the addition of sequencing grade-modified trypsin (Sigma-Aldrich) in an enzyme:protein ratio of 1:20, and samples were then incubated overnight at 37°C. The resulting tryptic peptides were labeled subsequently using the TMT-6 Plex Isobaric Mass Tagging Kit (Thermo Fisher Scientific) according to the manufacturer's instructions. After labeling, the samples were pooled, dried, and desalted using a SEP-PAK C18 Cartridge (Waters). Finally, the cleaned tryptic peptides were evaporated to dryness and stored at −20°C until further analysis.

Two-Dimensional Liquid Chromatography-Tandem Mass Spectrometry Analysis of Labeled Peptide Mixtures

The first dimension consisted of a separation by reverse-phase chromatography at basic pH with an Ultimate 3000 HPLC apparatus (Dionex) during which 30 fractions were collected. They were later alternatively combined into six fractions and, finally, offline injected into the tandem mass spectrometry system. The fractions were then divided into two aliquots for subsequent differential proteomics and phosphoproteomics.

Liquid Chromatography-Tandem Mass Spectrometry Triple Time of Flight Analysis of Nonphosphorylated Proteins

Peptide fractions were subjected to liquid chromatography-tandem mass spectrometry (LC-MS/MS) analysis using a nanoliquid chromatography system (Eksigent Technologies nanoLC Ultra 1D plus; AB Sciex) coupled to a high-speed Triple Time of Flight (TOF) 5600 mass spectrometer (AB Sciex) with a nanoelectrospray ion source. Samples were injected into a C18 PepMap trap column (5 μm, 100 μm i.d. × 2 cm; Thermo Fisher Scientific) at 2 μL min^{-1}, in 0.1% formic acid in water, and the trap column was switched online to a C18 nanoAcquity BEH analytical column (1.7 μm, 100 Å, 75 μm i.d. × 15 cm; Waters). Equilibration was done in mobile phase A (0.1% formic acid in water), and peptide elution was achieved in a 120-min linear gradient from 5% to 40% B (0.1% formic acid in acetonitrile) at 250 nL min^{-1}. The mass spectrometer was operated in a data-dependent acquisition mode. The accumulation time for the time of flight (TOF) scans was set to 250 ms, and up to 30 precursor ions were monitored per cycle.

LC-MS/MS Triple TOF Analysis of Phosphorylated Protein Fractions

Part of each fraction (75%) from the first chromatographic dimension was subjected to phosphopeptide purification. The enrichment procedure concatenates two in-house packed microcolumns, the IMAC microcolumn and the Oligo R3 reverse-phase column, that provide selective purification and sample cleanup prior to LC-MS/MS analysis, and was performed according to Navajas et al. (2011). After phosphopeptide enrichment, all the IMAC eluates from the six fractions were combined and subjected to LC-MS/MS triple TOF analysis, following a 220-min linear gradient and data-dependent acquisition mode, with the same parameters described above.

Proteomics Data Analysis

Tandem mass spectrometry spectra were exported to MGF format using Peak View version 1.2.0.3 (Sciex) and searched using Mascot Server 2.5.1, OMSSA 2.1.9, X!TANDEM 2013.02.01.1, and Myrimatch 2.2.140 against a composite target/decoy database built from the 31,551 sequences in the Arabidopsis reference proteome from the Uniprot Knowledgebase, together with commonly occurring contaminants. Search engines were configured to match potential peptide candidates with mass error tolerance of 25 ppm and fragment ion tolerance of 0.02 D, allowing up to two missed tryptic cleavage sites and a maximum isotope error (^{13}C) of 1, considering fixed methyl methanethiosulfonate modification of Cys and variable oxidation of Met, pyro-Glu from Gln or Glu at the peptide N terminus, and acetylation of the protein N terminus. Score distribution models were used to compute peptide spectrum match *P* values as described by Ramos-Fernández et al. (2008), and spectra recovered by a false discovery rate (FDR) ≤ 0.01 (peptide level) filter were selected for quantitative analysis. The approximately 4% of signals with the lowest quality were removed prior to further analysis. Differential regulation was measured using linear models (López-Serra et al., 2014), and statistical significance was measured using *q* values (FDR). All analyses were conducted using software from Proteobotics. The cutoff for differentially regulated proteins was established at FDR ≤ 2.7% and $\log_2$ ratios (plus-VC treatment versus minus-VC treatment) of either greater than 0.475 (for proteins whose expression is up-regulated by VCs) or less than −0.475 (for proteins whose expression is down-regulated by VCs).

Statistical Analysis

The data are presented as means ± SE of four independent experiments, with three to five replicates for each experiment. The significance of differences between nontreated plants and plants that were treated with VCs from *A. alternata* was statistically evaluated with Student's *t* test using SPSS software. Differences were considered significant at $P < 0.05$. The between-treatment differences in the hormone content analyses were evaluated by the one-way univariate ANOVA for parametric data and the Kruskal-Wallis *H* test for nonparametric data using the open source R software 2.15.1 (http://cran.r-project.org/). Multiple comparisons after ANOVA were calculated using the posthoc Tukey's honestly significant difference test.

Supplemental Data

The following supplemental materials are available.

Supplemental Figure S1. Free amino acid contents in the leaves of *pgi1-2* plants cultured in the absence or presence of *A. alternata* VCs for 3 d.

Supplemental Figure S2. VCs emitted by *A. alternata* promote the augmentation of CK levels in the leaves of *pgi1-2* plants.

Supplemental Figure S3. Categorization of the differentially expressed proteins in leaves of *pgi1-2* plants cultured in the presence of VCs emitted by *A. alternata* according to their subcellular localizations.

Supplemental Table S1. List of proteins whose expression is differentially regulated by VCs emitted by *A. alternata*.

Supplemental Table S2. List of proteins identified in the proteomic study.

Supplemental Table S3. Subcellular localizations and functions of the proteins differentially regulated by *A. alternata* VCs.

ACKNOWLEDGMENTS

We thank María Teresa Sesma, Maite Hidalgo, and Ohiana Cabodevilla (Institute of Agrobiotechnology of Navarra) for technical support.

Received June 20, 2016; accepted September 21, 2016; published September 23, 2016.

LITERATURE CITED

Bahaji A, Baroja-Fernández E, Ricarte-Bermejo A, Sánchez-López ÁM, Muñoz FJ, Romero JM, Ruiz MT, Baslam M, Almagro G, Sesma MT, et al (2015a) Characterization of multiple SPS knockout mutants reveals redundant functions of the four Arabidopsis sucrose phosphate synthase isoforms in plant viability, and strongly indicates that enhanced respiration and accelerated starch turnover can alleviate the blockage of sucrose biosynthesis. Plant Sci **238:** 135–147

Bahaji A, Baroja-Fernández E, Sánchez-López ÁM, Muñoz FJ, Li J, Almagro G, Montero M, Pujol P, Galarza R, Kaneko K, et al (2014a) HPLC-MS/MS analyses show that the near-starchless *aps1* and *pgm* leaves accumulate wild type levels of ADPglucose: further evidence for the occurrence of important ADPglucose biosynthetic pathway(s) alternative to the pPGI-pPGM-AGP pathway. PLoS ONE **9:** e104997

Bahaji A, Li J, Ovecka M, Ezquer I, Muñoz FJ, Baroja-Fernández E, Romero JM, Almagro G, Montero M, Hidalgo M, et al (2011) *Arabidopsis thaliana* mutants lacking ADP-glucose pyrophosphorylase accumulate starch and wild-type ADP-glucose content: further evidence for the occurrence of important sources, other than ADP-glucose pyrophosphorylase, of ADP-glucose linked to leaf starch biosynthesis. Plant Cell Physiol **52:** 1162–1176

Bahaji A, Li J, Sánchez-López ÁM, Baroja-Fernández E, Muñoz FJ, Ovecka M, Almagro G, Montero M, Ezquer I, Etxeberria E, et al (2014b) Starch biosynthesis, its regulation and biotechnological approaches to improve crop yields. Biotechnol Adv **32:** 87–106

Bahaji A, Sánchez-López ÁM, De Diego N, Muñoz FJ, Baroja-Fernández E, Li J, Ricarte-Bermejo A, Baslam M, Aranjuelo I, Almagro G, et al (2015b) Plastidic phosphoglucose isomerase is an important determinant of starch accumulation in mesophyll cells, growth, photosynthetic capacity, and biosynthesis of plastidic cytokinins in Arabidopsis. PLoS ONE **10:** e0119641

Baroja-Fernández E, Muñoz FJ, Zandueta-Criado A, Morán-Zorzano MT, Viale AM, Alonso-Casajús N, Pozueta-Romero J (2004) Most of ADP × glucose linked to starch biosynthesis occurs outside the chloroplast in source leaves. Proc Natl Acad Sci USA **101:** 13080–13085

Brenner WG, Schmülling T (2015) Summarizing and exploring data of a decade of cytokinin-related transcriptomics. Front Plant Sci **6:** 29

Cho MH, Lim H, Shin DH, Jeon JS, Bhoo SH, Park YI, Hahn TR (2011) Role of the plastidic glucose translocator in the export of starch degradation products from the chloroplasts in *Arabidopsis thaliana*. New Phytol **190:** 101–112

Ditengou FA, Müller A, Rosenkranz M, Felten J, Lasok H, van Doorn MM, Legué V, Palme K, Schnitzler JP, Polle A (2015) Volatile signalling by sesquiterpenes from ectomycorrhizal fungi reprogrammes root architecture. Nat Commun **6:** 6279

Ezquer I, Li J, Ovecka M, Baroja-Fernández E, Muñoz FJ, Montero M, Díaz de Cerio J, Hidalgo M, Sesma MT, Bahaji A, et al (2010) Microbial volatile emissions promote accumulation of exceptionally high levels of starch in leaves in mono- and dicotyledonous plants. Plant Cell Physiol **51:** 1674–1693

Fic E, Kedracka-Krok S, Jankowska U, Pirog A, Dziedzicka-Wasylewska M (2010) Comparison of protein precipitation methods for various rat brain structures prior to proteomic analysis. Electrophoresis **31:** 3573–3579

Frentzen M (2004) Phosphatidylglycerol and sulfoquinovosyldiacylglycerol: anionic membrane lipids and phosphate regulation. Curr Opin Plant Biol **7:** 270–276

Fristedt R, Willig A, Granath P, Crèvecoeur M, Rochaix JD, Vener AV (2009) Phosphorylation of photosystem II controls functional macroscopic folding of photosynthetic membranes in *Arabidopsis*. Plant Cell **21:** 3950–3964

Giese JO, Herbers K, Hoffmann M, Klösgen RB, Sonnewald U (2005) Isolation and functional characterization of a novel plastidic hexokinase from *Nicotiana tabacum*. FEBS Lett **579:** 827–831

Gonzalez-Jorge S, Ha SH, Magallanes-Lundback M, Gilliland LU, Zhou A, Lipka AE, Nguyen YN, Angelovici R, Lin H, Cepela J, et al (2013) *Carotenoid cleavage dioxygenase4* is a negative regulator of β-carotene content in *Arabidopsis* seeds. Plant Cell **25:** 4812–4826

He Y, Chen L, Zhou Y, Mawhinney TP, Chen B, Kang BH, Hauser BA, Chen S (2011) Functional characterization of *Arabidopsis thaliana* isopropylmalate dehydrogenases reveals their important roles in gametophyte development. New Phytol **189:** 160–175

Helliwell CA, Sullivan JA, Mould RM, Gray JC, Peacock WJ, Dennis ES (2001) A plastid envelope location of Arabidopsis ent-kaurene oxidase links the plastid and endoplasmic reticulum steps of the gibberellin biosynthesis pathway. Plant J **28:** 201–208

Humplík JF, Bergougnoux V, Jandová M, Šimura J, Pěnčík A, Tomanec O, Rolčík J, Novák O, Fellner M (2015) Endogenous abscisic acid promotes hypocotyl growth and affects endoreduplication during dark-induced growth in tomato (*Solanum lycopersicum* L.). PLoS ONE **10:** e0117793

Hung R, Lee S, Bennett JW (2013) *Arabidopsis thaliana* as a model system for testing the effect of Trichoderma volatile organic compounds. Fungal Ecol **6:** 19–26

Hunt PW, Klok EJ, Trevaskis B, Watts RA, Ellis MH, Peacock WJ, Dennis ES (2002) Increased level of hemoglobin 1 enhances survival of hypoxic stress and promotes early growth in *Arabidopsis thaliana*. Proc Natl Acad Sci USA **99:** 17197–17202

Hunt PW, Watts RA, Trevaskis B, Llewelyn DJ, Burnell J, Dennis ES, Peacock WJ (2001) Expression and evolution of functionally distinct haemoglobin genes in plants. Plant Mol Biol **47:** 677–692

Imhof J, Huber F, Reichelt M, Gershenzon J, Wiegreffe C, Lächler K, Binder S (2014) The small subunit 1 of the *Arabidopsis* isopropylmalate isomerase is required for normal growth and development and the early stages of glucosinolate formation. PLoS ONE **9:** e91071

Kammerer B, Fischer K, Hilpert B, Schubert S, Gutensohn M, Weber A, Flügge UI (1998) Molecular characterization of a carbon transporter in plastids from heterotrophic tissues: the glucose 6-phosphate/phosphate antiporter. Plant Cell **10:** 105–117

Kanchiswamy CN, Malnoy M, Maffei ME (2015) Chemical diversity of microbial volatiles and their potential for plant growth and productivity. Front Plant Sci **6:** 151

Kaplan F, Guy CL (2004) β-Amylase induction and the protective role of maltose during temperature shock. Plant Physiol **135:** 1674–1684

Kieber JJ, Schaller GE (2014) Cytokinins. The Arabidopsis Book **12:** e0168 doi/10.1199/tab.0168

Ko D, Kang J, Kiba T, Park J, Kojima M, Do J, Kim KY, Kwon M, Endler A, Song WY, et al (2014) *Arabidopsis* ABCG14 is essential for the root-to-shoot translocation of cytokinin. Proc Natl Acad Sci USA **111:** 7150–7155

Kunz HH, Häusler RE, Fettke J, Herbst K, Niewiadomski P, Gierth M, Bell K, Steup M, Flügge UI, Schneider A (2010) The role of plastidial glucose-6-phosphate/phosphate translocators in vegetative tissues of *Arabidopsis thaliana* mutants impaired in starch biosynthesis. Plant Biol (Stuttg) (Suppl 1) **12:** 115–128

Lazár D (2015) Parameters of photosynthetic energy partitioning. J Plant Physiol **175:** 131–147

Li J, Ezquer I, Bahaji A, Montero M, Ovecka M, Baroja-Fernández E, Muñoz FJ, Mérida A, Almagro G, Hidalgo M, et al (2011) Microbial volatile-induced accumulation of exceptionally high levels of starch in Arabidopsis leaves is a process involving NTRC and starch synthase classes III and IV. Mol Plant Microbe Interact **24:** 1165–1178

Lichtenthaler HK (1987) Chlorophylls and carotenoids: pigments of photosynthetic biomembranes. Methods Enzymol **148:** 350–382

Loiret FG, Grimm B, Hajirezaei MR, Kleiner D, Ortega E (2009) Inoculation of sugarcane with Pantoea sp. increases amino acid contents in shoot tissues: serine, alanine, glutamine and asparagine permit concomitantly ammonium excretion and nitrogenase activity of the bacterium. J Plant Physiol **166:** 1152–1161

López-Serra P, Marcilla M, Villanueva A, Ramos-Fernandez A, Palau A, Leal L, Wahi JE, Setien-Baranda F, Szczesna K, Moutinho C, et al (2014) A DERL3-associated defect in the degradation of SLC2A1 mediates the Warburg effect. Nat Commun **5:** 3608

Lytovchenko A, Bieberich K, Willmitzer L, Fernie AR (2002) Carbon assimilation and metabolism in potato leaves deficient in plastidial phosphoglucomutase. Planta **215:** 802–811

Navajas R, Paradela A, Albar JP (2011) Immobilized metal affinity chromatography/reversed-phase enrichment of phosphopeptides and analysis by CID/ETD tandem mass spectrometry. Methods Mol Biol **681:** 337–348

Novák O, Hauserová E, Amakorová P, Doležal K, Strnad M (2008) Cytokinin profiling in plant tissues using ultra-performance liquid chromatography-electrospray tandem mass spectrometry. Phytochemistry **69:** 2214–2224

Ovecka M, Bahaji A, Muñoz FJ, Almagro G, Ezquer I, Baroja-Fernández E, Li J, Pozueta-Romero J (2012) A sensitive method for confocal fluorescence microscopic visualization of starch granules in iodine stained samples. Plant Signal Behav **7:** 1146–1150

Peñuelas J, Asensio D, Tholl D, Wenke K, Rosenkranz M, Piechulla B, Schnitzler JP (2014) Biogenic volatile emissions from the soil. Plant Cell Environ **37:** 1866–1891

Pokhilko A, Bou-Torrent J, Pulido P, Rodríguez-Concepción M, Ebenhöh O (2015) Mathematical modelling of the diurnal regulation of the MEP pathway in *Arabidopsis*. New Phytol **206:** 1075–1085

Pozueta-Romero J, Ardila F, Akazawa T (1991) ADP-glucose transport by the chloroplast adenylate translocator is linked to starch biosynthesis. Plant Physiol **97:** 1565–1572

Pulido P, Perello C, Rodriguez-Concepcion M (2012) New insights into plant isoprenoid metabolism. Mol Plant **5:** 964–967

Quick WP, Scheibe R, Neuhaus HE (1995) Induction of hexose-phosphate translocator activity in spinach chloroplasts. Plant Physiol **109:** 113–121

Ramos-Fernández A, Paradela A, Navajas R, Albar JP (2008) Generalized method for probability-based peptide and protein identification from tandem mass spectrometry data and sequence database searching. Mol Cell Proteomics **7:** 1748–1754

Riefler M, Novak O, Strnad M, Schmülling T (2006) *Arabidopsis* cytokinin receptor mutants reveal functions in shoot growth, leaf senescence, seed size, germination, root development, and cytokinin metabolism. Plant Cell **18:** 40–54

Ruiz-Sola MÁ, Rodríguez-Concepción M (2012) Carotenoid biosynthesis in Arabidopsis: a colorful pathway. The Arabidopsis Book **10:** e0158 doi/10.1199/tab.0158

Ryu CM, Farag MA, Hu CH, Reddy MS, Wei HX, Paré PW, Kloepper JW (2003) Bacterial volatiles promote growth in Arabidopsis. Proc Natl Acad Sci USA **100:** 4927–4932

Sánchez-López ÁM, Baslam M, De Diego N, Muñoz FJ, Bahaji A, Almagro G, Ricarte-Bermejo A, García-Gómez P, Li J, Humplík JF, et al (2016) Volatile compounds emitted by diverse phytopathogenic microorganisms promote plant growth and flowering through cytokinin action. Plant Cell Environ (in press) 10.1111/pce.12759

Sønderby IE, Geu-Flores F, Halkier BA (2010) Biosynthesis of glucosinolates: gene discovery and beyond. Trends Plant Sci **15:** 283–290

Tantikanjana T, Mikkelsen MD, Hussain M, Halkier BA, Sundaresan V (2004) Functional analysis of the tandem-duplicated P450 genes SPS/BUS/CYP79F1 and CYP79F2 in glucosinolate biosynthesis and plant development by *Ds* transposition-generated double mutants. Plant Physiol **135:** 840–848

Tantikanjana T, Yong JWH, Letham DS, Griffith M, Hussain M, Ljung K, Sandberg G, Sundaresan V (2001) Control of axillary bud initiation and shoot architecture in Arabidopsis through the SUPERSHOOT gene. Genes Dev **15:** 1577–1588

Vogt AM, Ackermann C, Noe T, Jensen D, Kübler W (1998) Simultaneous detection of high energy phosphates and metabolites of glycolysis and the Krebs cycle by HPLC. Biochem Biophys Res Commun **248:** 527–532

Weber A, Servaites JC, Geiger DR, Kofler H, Hille D, Gröner F, Hebbeker U, Flügge UI (2000) Identification, purification, and molecular cloning of a putative plastidic glucose translocator. Plant Cell **12:** 787–802

Weikl F, Ghirardo A, Schnitzler JP, Pritsch K (2016) Sesquiterpene emissions from *Alternaria alternata* and *Fusarium oxysporum:* effects of age, nutrient availability, and co-cultivation. Sci Rep **6:** 22152

Weise SE, Schrader SM, Kleinbeck KR, Sharkey TD (2006) Carbon balance and circadian regulation of hydrolytic and phosphorolytic breakdown of transitory starch. Plant Physiol **141:** 879–886

Werner T, Holst K, Pörs Y, Guivarc'h A, Mustroph A, Chriqui D, Grimm B, Schmülling T (2008) Cytokinin deficiency causes distinct changes of sink and source parameters in tobacco shoots and roots. J Exp Bot **59:** 2659–2672